Growth of Eu on Pd(111) studied by x-ray and uv photoemission and crystallographic properties as determined by reflection-high-energy-electron-diffraction and x-ray-diffraction studies

F. Bertran, T. Gourieux, and G. Krill
Laboratoire de Physique des Solides, Université de Nancy I, Boîte Postale No. 239, 54506 Vandoeuvre-lès-Nancy, France

M. F. Ravet-Krill
Laboratoire Mixte CNRS Saint Gobain, Boîte Postale No. 109, 54704 Pont-à-Mousson CEDEX, France
and Laboratoire de Microstructures et de Microélectronique, 196 Avenue Henri Ravera, 92220 Bagneux, France

M. Alnot and J. J. Ehrhardt
Laboratoire Maurice Letort, Route de Vandoeuvre, 54600 Villers-lès-Nancy, France

W. Felsch
I. Physikalisches Institut, Universität Göttingen, Bunsenstrasse 9, 3400 Göttingen, Germany
(Received 30 January 1992)

The electronic properties of europium layers deposited on a Pd(111) single crystal (up to 190 Å of europium) have been studied by ultraviolet and x-ray photoemission spectroscopies on both the valence bands and core levels (Eu and Pd). It is shown that, except for very low europium thicknesses, the formation of the Eu/Pd(111) interface is dominated by diffusion processes between europium and palladium. A systematic comparison between the electronic properties of this diffusive interface and the ones of well-defined intermetallic compounds ($EuPd_5$, $EuPd_3$, $EuPd_2$, and EuPd) and amorphous Eu_xPd_{1-x} alloys, allows one to specify what kind of alloys or compounds formed at the interface as a function of the Eu thickness and/or temperature. Here, benefit is taken from the well-known sensitivity of the Eu valence to local environment. The most interesting result of this study is that these highly disordered Eu/Pd interfaces can be crystallized by heating the layers at moderate temperatures (800–1000 K), or by performing the evaporations of Eu on the Pd(111) substrate held at similar temperatures. *In all cases* and for all Eu thicknesses, reflection high-energy electron diffraction, x-ray diffraction, and photoemission experiments show evidence of the epitaxy of a *trivalent,* most likely $EuPd_3$, intermetallic compound on the Pd(111) surface. Moreover, the epitaxial growth of Pd(111) on this trivalent compound is possible. It opens the possibility of building a metallic superlattice such as $Pd/EuPd_3$.

I. INTRODUCTION

In the past few years, numerous studies have been devoted to the determination of the growth mechanisms of rare-earth (RE) elements on transition metals (TM).[1–14] The principal aim of such studies is to determine, as precisely as possible, all the properties of the interfaces that are formed between RE and TM elements, in order to investigate the possibility of building artificial modulated structures (multilayers and/or superlattices) presenting interesting physical properties. In the case of RE-TM systems, the interest is obviously related to the exotic magnetic properties which can be obtained in such materials. In particular, as it is commonly realized today in the case of semiconductor superlattices, the possibility of achieving TM/RE-TM (compound) metallic superlattices needs to be investigated. Recently, bidimensional growth of intermetallic RE-TM compounds on TM, obtained by coevaporation [Yb_2Ni, $YbNi_2$ on Mo(110)] (Ref. 5) has been demonstrated. Similarly, it has been shown that tridimensional growth of RE-TM *compounds* on TM can occur in several systems where strong diffusion takes place between the RE and the TM element [e.g., Yb/Ni(100),[4] Nd/Cu(100), Nd/Cu(111),[13] etc.]

In this paper, we present the results we obtained on the Eu-Pd system, for Eu coverages up to 190 Å. The growth mechanism and electronic properties are followed by photoemission [x-ray photoemission spectroscopy (XPS) and ultraviolet photoemission spectroscopy (UPS)] and Auger spectroscopy (AES), whose surface sensitivity is well known. The structural properties are studied by reflection-high-energy-electron-diffraction (RHEED) and x-ray-diffraction experiments.

The Eu-Pd system has been chosen for the following reasons.

(i) From earlier experiments,[15] the possibility of obtaining amorphous Eu_xPd_{1-x} alloys on a wide range of concentration ($0.15 \leq x \leq 0.5$) has been established and the study of their electronic properties has revealed the continuous change in Eu valence ($Eu^{3+}[4f^6(5d6s)^3]$ to $Eu^{2+}[4f^7(5d6s)^2]$) with a transition at $x=0.3$ and which reflects the modification in the local environment of Eu by Pd atoms.

(ii) Around this valence transition, several intermetallic compounds are known to exist in the Eu-Pd phase diagram: $EuPd_5$ ($SmPt_5$ structure) and $EuPd_3$ ($AuCu_3$ structure) in the trivalent state, $EuPd_2$ ($MgCu_2$ structure) and EuPd (BCr structure) in the divalent state.

(iii) The interdiffusion between europium and palladium is known to be very important. For instance, europium and palladium interdiffuse even at low temperature (down to 77 K), which is not generally the case for other rare-earth–transition-metal systems.

In Sec. II, we shall describe the experimental techniques we use both to prepare the Eu/Pd interfaces and to study them. In Sec. III, the structural information obtained from RHEED and x-ray-diffraction experiments will be presented. We shall focus essentially on the results that demonstrate the formation of an epitaxial growth of a slightly distorted $EuPd_3$ intermetallic compound on Pd(111). Then we shall demonstrate that epitaxy is preserved when Pd is evaporated on this epitaxial compound. Section IV will be devoted to the presentation of the results obtained on the electronic structure of these Eu/Pd interfaces from photoemission experiments (XPS and UPS), and comparison with those of polycrystalline $EuPd_y$ ($y=1, 2, 3, 5$) compounds will be made. Finally, the main conclusions of our study will be given in Sec V.

II. EXPERIMENTAL DETAILS

A. Evaporation of Eu on Pd(111)

The evaporations of europium and palladium were made in a molecular-beam-epitaxy (MBE)-like the ultrahigh-vacuum chamber built by MECA 2000 (France).[16] This MBE chamber is directly connected to standard photoemission equipment from VG Scientific (England) (VG ESCALAB II). The base pressure in the two chambers is typically in the 5×10^{-11}-hPa range. In the MBE chamber, a cryogenic shield cooled to liquid-nitrogen temperature allows one to perform the evaporations at low pressure.

The europium depositions were made by using a Knudsen cell with a boron nitride crucible operating at 800 K. The pressure during the evaporations was always less than 5×10^{-9} hPa. Palladium was evaporated by electron bombardment at a temperature of 1900 K under a pressure of 10^{-10} hPa. The evaporation rates were continuously measured by two water-cooled quartz microbalances from INFICON. The evaporation rates used for our studies were in the range of one monolayer (ML) per minute and the error arising from the quartz monitors themselves can be estimated at 10%.

B. Structural studies

The RHEED experiments were performed *in situ* with a VG LEG 300 apparatus working at 20 keV under a 1° incidence. X-ray-diffraction experiments were performed *ex situ* on a PHILIPS High Resolution Diffractometer. This setup is suitable for reflectometry and studies of epitaxial systems.[17] A Ge(220) four-crystal monochromator delivers pure $CoK\alpha_1$ radiation ($\lambda=1.78892$ Å with $\Delta\lambda/\lambda=2.3\times10^{-5}$) and a parallel beam (divergence $\Delta\omega=0.07$ mrad).[18] We have recorded diffraction diagrams in the $\theta/2\theta$ scan and 2θ scan modes with a 2θ step of 0.02°, a counting time of 8 sec/step, and a receiving slit of 0.3°. The rocking curves were scanned in the ω scan mode with a step of 0.01°, a counting time of 2 sec/step, and an acceptance angle of 4° for the detector kept in the Bragg fixed position.

C. Spectroscopic studies

The Auger spectra were recorded in the derivative mode with an AES spectrometer from RIBER (France) (OPC105) working at 2 keV with an emission current of 2 μA. The modulation was 2 V peak to peak and the total resolution in energy ($\Delta E/E$) in the 5×10^{-3} range. The XPS spectra were obtained using the Al Kα radiation ($h\nu=1486.6$ eV) and the UPS ones with the He I ($h\nu=21.2$ eV) and He II ($h\nu=40.8$ eV) radiations, the energy resolution being ≈1.0 eV for XPS and ≈0.2 eV for UPS.

D. Samples

The substrate used for our depositions was a Pd(111) single crystal (8 mm in diameter and 0.5 mm in thickness). Before each deposition, it was cleaned by argon ion bombardment at a temperature of 900 K and then heated again at 900 K for 10 min until no traces of contamination (O, C, S, etc.) could be detected by AES. Moreover, we checked carefully that the recrystallization was fully achieved by doing RHEED experiments.

The polycrystalline samples $EuPd_5$, $EuPd_3$, $EuPd_2$, and EuPd were obtained by arc melting starting from 5*N* Pd and 3*N* Eu. X-ray-diffraction experiments were performed on all samples in order to check that they were all single phased [for $EuPd_5$, a small amount ($\approx5\%$) of parasitic phase was present].

In the case of the x-ray-diffraction studies, which were performed *ex situ*, the samples were covered by a 40-Å Pd layer deposited at $T=300$ K, in order to avoid any problem of contamination (oxidation, etc.).

III. STRUCTURAL STUDIES

A. RHEED Experiments

The RHEED patterns were obtained for three different azimuths of the Pd(111) substrate, namely the $[01\bar{1}]$, $[\bar{2}11]$, and $[\bar{3}21]$ directions. Because the results are similar for the three azimuths, we report only, in Fig. 1, the RHEED patterns obtained in the $[01\bar{1}]$ direction.

In Fig. 1(a), the diffraction lines are those characteristic of the $p(1\times1)$ structure ($d=2.75$ Å) of pure Pd(111). In Fig. 1(b), we show the results obtained for a 3-Å europium deposit (i.e., for a coverage $\Theta\approx1.5$; see Sec. IV A for the definition of Θ) at room temperature (RT). A well-ordered $p(2\times2)$ structure ($d=5.50$ Å), with no change in the Pd interatomic distances (in the limit of accuracy: ±0.1 Å), is observed. The $p(2\times2)$ structure is visible for $0.5\leq\Theta\leq2.3$ (i.e., up to nearly 5 Å Eu deposit), but with an increasing diffuse background when Θ becomes higher than 2. For thicker Eu layer deposition at RT, as shown in Fig. 1(c), we rapidly lose all the diffraction lines, which indicates that the surface becomes strongly disordered. This situation reflects, as we shall discuss later, the occurrence of interdiffusion between Eu and Pd.

The interesting point is the result we obtain when the samples are annealed between 800 and 1000 K, or if the Eu deposit is made within this temperature range. As shown in Fig. 1(d), which corresponds to a 190-Å Eu RT deposit annealed for 2 min at 1000 K, we get again the $p(2\times2)$ diffraction lines. Note that (i) in the limit of accuracy, the surface lattice parameter (5.50±0.1 Å) is found to be twice that of Pd(111) and (ii) this situation is *independent of the thickness of deposited Eu.* This result strongly suggests the formation of an epitaxial Eu-Pd compound on the Pd(111) substrate. We shall see that all our results confirm this hypothesis. It is difficult, perhaps even impossible, from the RHEED results alone to obtain the structure of this epitaxial compound; the fact that, at the surface, the divalent state of Eu is always stabilized may obscure the conclusion. Nevertheless, it is clear from these RHEED results that we deal with a hexagonal surface lattice where the in-plane parameter d is about 5.50 Å. Among *all the known* intermetallic Eu-Pd compounds, the only possible candidates are (i) (111) $EuPd_3$ ($AuCu_3$ structure) with $d=a\sqrt{2}=5.80$ Å; (ii) (111) $EuPd_2$ ($MgCu_2$ structure) with $d=a/\sqrt{2}=5.49$ Å. The results we obtained by x-ray diffraction will clarify, more or less, the situation.

Another interesting point is illustrated in Fig. 1(e): the RHEED diffraction pattern corresponds to the situation shown in Fig. 1(d), where an additional amount of 40-Å Pd has been deposited at RT, followed by an annealing of 2 min at 700 K. We clearly observe again the $p(1\times1)$ structure of pure Pd(111) showing that Pd grows epitaxially on the former Eu-Pd compound.

B. X-ray-diffraction results

X-ray-diffraction experiments were performed on the annealed Eu/Pd(111) interface (Eu deposited thickness: 190 Å). As shown in Fig. 2(a), only Bragg peaks of the (111) family of the cubic structure can be observed on the

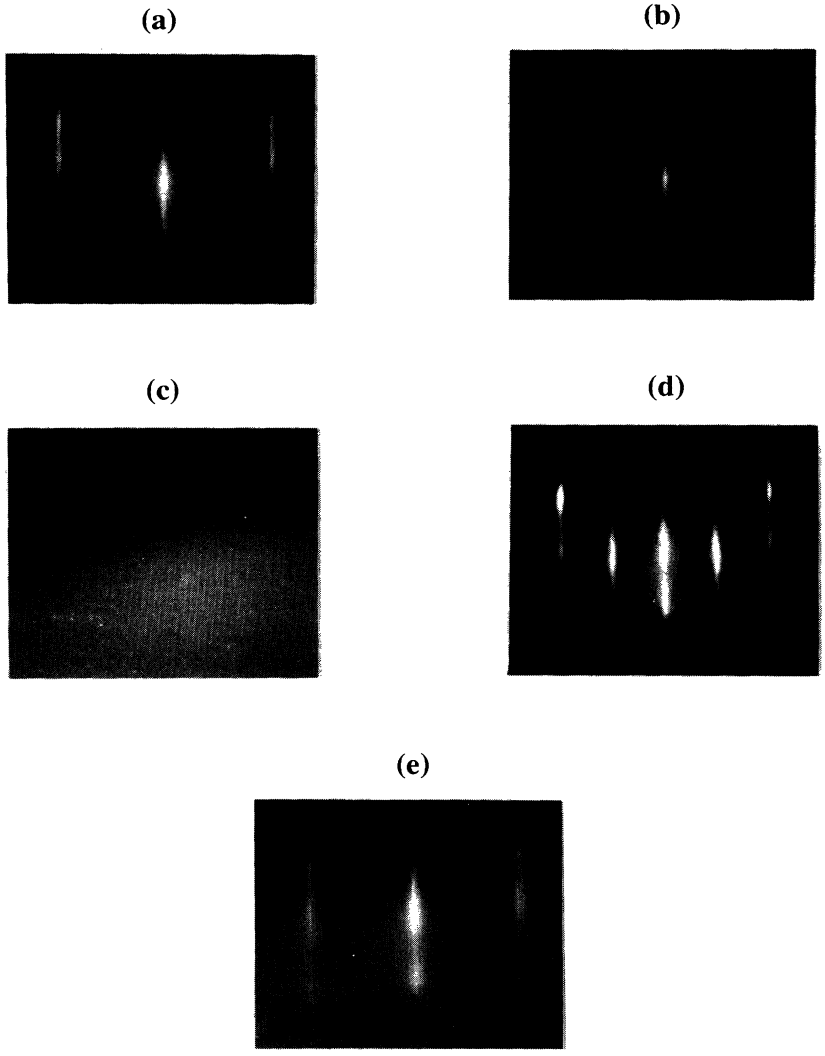

FIG. 1. RHEED patterns in the [01$\bar{1}$] real-space direction. (a) pure Pd(111). (b) 3-Å Eu deposited at RT. (c) Disappearance of RHEED patterns when the Eu deposit at RT is higher than 5 Å. (d) 190-Å Eu deposited at RT and annealed for 2 min at 1000 K. (e) 40-Å Pd deposited on the 190-Å reconstructed interface and annealed for 2 min at 700 K.

$\theta/2\theta$ scan diffractograms, which means that only these planes are parallel to the sample surface. In fact, each peak of the monocrystalline Pd(111) substrate is accompanied by an equivalent peak of the alloyed-phase Eu-Pd, which is an indication of a very well-oriented structure. For simplicity, we have indexed the peaks of the alloyed phase as Eu-Pd(111) and Eu-Pd(222). The interplanar distance $d_{Pd}=2.2460\pm0.0005$ Å has been deduced from the position of the Pd(111) and Pd(222) peaks. The lattice parameter given by $a=d_{Pd}\sqrt{3}$ is in good agreement with the value given for pure palladium by the Joint Committee For Powder Diffraction Standard. The average interplanar distance in the growth direction for the alloyed phase was evaluated to be $d_{Eu\text{-}Pd}=2.2783\pm0.0005$ Å. A very weak additional peak at $2\theta=51.23°$, corresponding to $d=2.07$ Å, could be attributed to a residual twin in the layer.

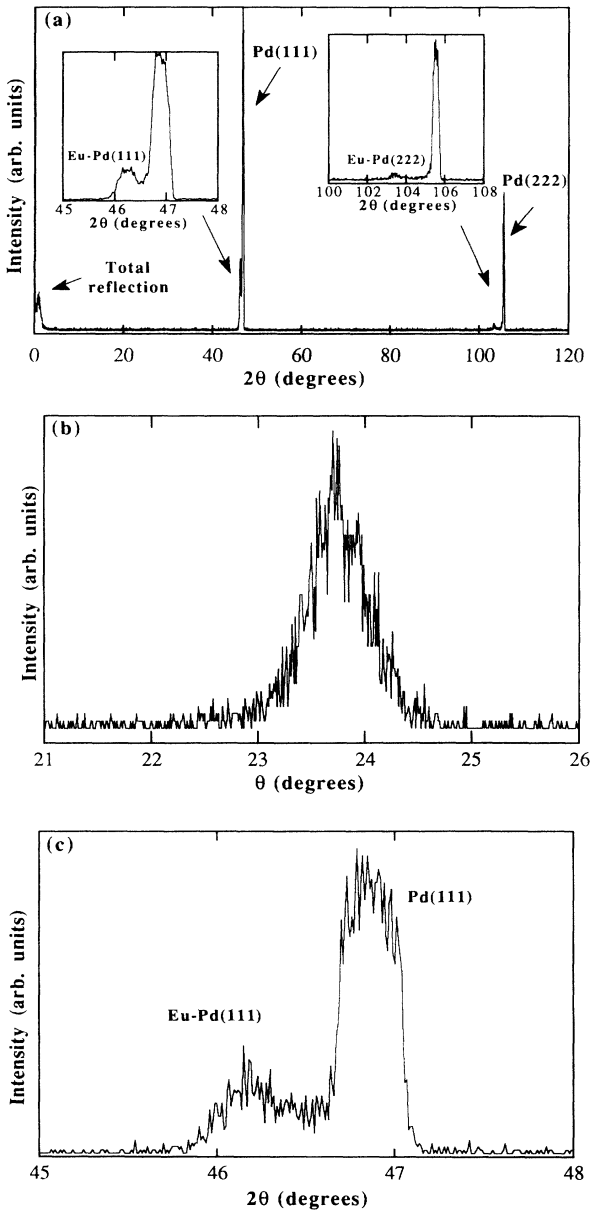

FIG. 2. X-ray-diffraction data obtained from the annealed sample. (a) $\theta/2\theta$ scan (see text). (b) Rocking curve around the [111] axis. The full width at half maximum is near 1°. (c) Dispersion of the (111) Bragg peak with 2θ (see text).

The rocking curves around the [111] axis recorded in the ω scan mode for several rotation angles (R) reveal in every case a full width at half maximum (FWHM) of $\Delta\omega\approx1°$, both for the palladium substrate and the alloyed layer [Fig. 2(b)]. It means that the mosaicity of the deposited film and the substrate are of the same order of magnitude. However, the maximum of the rocking curve for the Eu-Pd(111) axis shifts around the Pd(111) axis when the angle R is changed. This indicates a disorientation of the axes with respect to each other, which could be due to defects generated by the growth mechanisms.[19] Cross-sectional transmission electron microscopy would be able to provide further information on that phenomenon.

By choosing an R angle for which the rocking curves of Pd and Eu-Pd were mixed up, i.e., when both diffraction vectors were lying in the goniometric circle plane, and by fixing the incident angle ω given by the maximum of the rocking curve, we have achieved 2θ scans for the (111) Bragg peaks, with the aim of evaluating the distribution of the interplanar distances. The low value of the FWHM ($\Delta2\theta=0.2°$) [Fig. 2(c)], for the Eu-Pd alloyed phase, similar to the one of the palladium substrate, indicates that the interplanar distances are weakly dispersed and close to a mean value $d=2.28\pm0.01$ Å. However, the observation of the (222) peaks, which is more accurate because of the higher angle of dispersion, hints at a diffraction contribution just between the Pd(222) and Eu-Pd(222) peaks, coming from a low proportion of intermediate interplanar distances, probably due to the strains at the interface between the palladium substrate and the Eu-Pd layer.

These x-ray-diffraction experiments show that, in the case discussed here, a well-ordered intermetallic Eu-Pd compound of "large" thickness ($e>190$ Å) grows *epitaxially* on the Pd(111) surface. It cannot be ($MgCu_2$-structure) $EuPd_2$, because the (111) reflection is extinguished in this structure. Thus the main peak at 23.12° ($d=2.277$ Å) would correspond to a (222) reflection. The second peak at 51.68° ($d=1.140$ Å) cannot be indexed in this structure; moreover, as discussed in Sec. IV, our XPS results show clearly that the Eu ions in this compound have to be trivalent, which is not the case for Eu(2+) in $EuPd_2$. The case of (trivalent) $EuPd_3$ with the cubic $AuCu_3$ structure is more interesting. Indeed, the distance between the (111) planes in this structure is 2.37 Å, as deduced from the lattice constant ($a=4.101$ Å). Similarly, the in-plane distance is 5.8 Å. The two diffraction lines we observed are correctly indexed in this structure as (111) and (222) reflections. The distance between the (111) planes (2.28 Å) corresponds to an in-plane distance of $d=\sqrt{2}\times\sqrt{3}\times d(111)=5.58$ Å, which is in good agreement with the RHEED results. However, we notice that it implies a 5% contraction in the interatomic distances both in and between the (111) planes and thus the compound has to match this strain on a large scale, which is quite surprising for an intermetallic compound.

Off-stoichiometry effects, which exist in $EuPd_3$ (Ref. 20) on a limited range of concentration (24–26 % in Eu), can change the lattice constant by an amount of ±0.02 Å, which is not enough to explain the contraction (in the 0.1/0.2-Å range) we observe here. From these diffraction experiments, we are not able to go further with this problem. Complementary investigations on in-plane and asymmetrical-plane distances, which need to be performed on much larger samples in order to allow low-angle experiments, are absolutely mandatory if we want to obtain an exact knowledge of the crystallographic structure. For our purpose, the main point is that we have to deal with an intermetallic compound that is quite close to $EuPd_3$ with the $AuCu_3$ structure.

IV. ELECTRONIC STRUCTURES AS STUDIED BY XPS, UPS, AND AES EXPERIMENTS

From the results presented in the above section, it appears that the growth mechanism of Eu/Pd interfaces can be described in three main steps. (1) The formation of a thin $p(2\times2)$ Eu layer at very low Eu coverage (typically $\leq 2-3$ ML). (2) The formation of disordered Eu-Pd layers for thicker Eu coverage (up to 190 Å). (3) The ordering of these Eu-Pd layers that form, at moderate temperatures (≈ 820 K), an epitaxial $EuPd_3$ compound on Pd(111).

In this section we shall present the results concerning the electronic properties of these Eu/Pd interfaces in the three regions described above.

A. Low-europium coverages (≤ 2 ML) grown at room temperature

Auger intensities obtained in that range of coverage are presented in Fig. 3. Despite the dispersion, a rather well-defined break is observed for the intensity of the Eu signal at an amount of evaporated Eu corresponding to $N_{Eu}=4\times10^{14}$ atoms/cm^2. We notice also the existence of a similar, but weaker, behavior on the Pd intensity at the same value of N_{Eu} that corresponds to a coverage of $\Theta\approx1$, i.e., to the completion of the $p(2\times2)$ layer of Eu on the Pd(111) substrate ($\Theta=1$ ML$=\frac{1}{4}\times15.4\times10^{14}$ atoms/cm^2). Thus, both AES and RHEED experiments support a layer-by-layer growth of Eu. Confirmation of this hypothesis is given by the UPS and XPS measurements, as well as from the analysis of the fine structure of AES signals. In Fig. 4, He II spectra are reported for clean Pd(111) and deposits of Eu on Pd(111) up to 3.5 ML. The kinetic energy of the emitted electrons in He II corresponds to a very small escape depth (≈ 4 Å), so that most of the emitted signal is due to the superficial layer(s). The sharp feature close to the Fermi level observed for the Pd(111) substrate is characteristic of a surface state of Pd (Ref. 21) and, as expected, its intensity is highly sensitive to the presence of any adsorbate on the surface. On the basis of the results presented in Fig. 4, we can conclude again that the Pd(111) surface is fully covered after the deposition of $N_{Eu}=4\times10^{14}$ atoms/cm^2, which corresponds to $\Theta\approx1$. The feature that appears below the Fermi energy (≈ 1.5 eV) is attributed to the Eu $4f$ states. Unlike these UPS spectra, the Pd Auger $M_{4,5}VV$ spectra are insensitive to the Eu coverage up to $\Theta=2$.[22] Similar results are deduced from the comparison of XPS Pd core-level spectra, which are not shown here. Thus, we conclude that, in this range of coverage, there is no strong interaction between europium and palladium and that no diffusion process takes place. This conclusion is reinforced by the results we obtained on the Eu $4d$ core-level spectra, which are shown in Fig. 5. For comparison, the Eu metal spectrum is also presented. Such spectra are made essentially of two well-resolved features arising from $^7D_{J=1,\ldots,5}$ and $^9D_{J=2,\ldots,6}$ spectroscopic final states in L-S notation. For the low-europium coverage case (i.e., $\Theta<2$ ML), it is clear that the Eu $4d$ spectra compare well with that of pure divalent Eu metal and we believe that the energy shift we observe (≈ 1.1 eV), is characteristic of isolated Eu atoms at the Pd(111) surface.

Obviously, it appears directly from Figs. 1, 3, and 5 that the situation corresponding to this $p(2\times2)$ arrange-

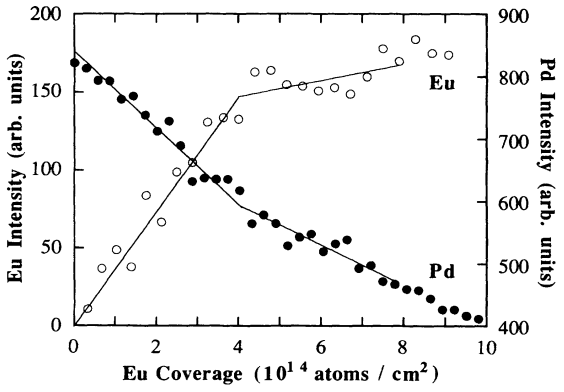

FIG. 3. Pd (MVV) and Eu (NVV) Auger intensities as a function of Eu coverage expressed in units of 10^{14} atoms/cm^2. The breaks in the curves corresponds to $\Theta\approx1$ as defined in Sec. IV A.

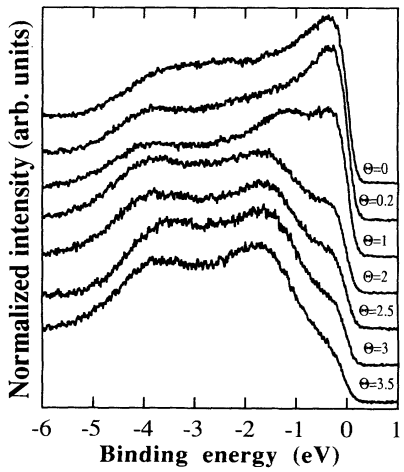

FIG. 4. He II spectra obtained at different Eu coverages. The spectra have been normalized to the maximum height.

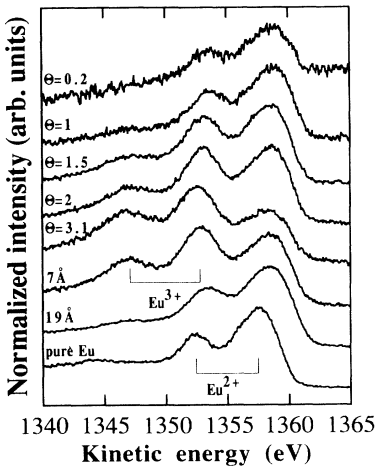

FIG. 5. Normalized (to the maximum height) Eu 4*d* XPS spectra for different Eu coverages expressed in units of Θ for the low values, then in Å for higher coverages (see text).

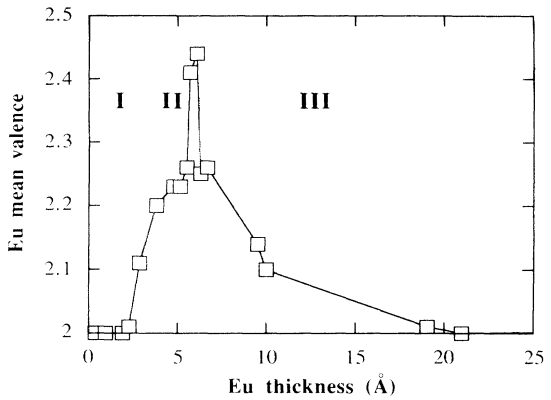

FIG. 6. Eu mean valence deduced from Eu 3*d* XPS spectra as a function of the Eu deposited thickness. Region I—epitaxy; region II—beginning of the diffusion regime; region III—diffusion regime.

ment of europium atoms is no longer stable for $\Theta \geq 2$ ML. We shall discuss this case in the next section.

B. High-europium coverages of the Pd(111) surface at room temperature

After the completion of the second $p(2\times2)$ layer of europium, we have shown in Sec. III that the RHEED patterns become more and more diffuse and finally disappear for $\Theta \approx 2.3$, indicating that the interface becomes more and more disordered. The loss of the RHEED pattern is directly correlated with the appearance of trivalent features on the 3*d* and 4*d* Eu XPS spectra (see Fig. 5). The Eu mean valence derived[32] from these spectra (Fig. 6) shows a pronounced maximum near $\Theta \approx 3$ (i.e., 6 Å). Then, it decreases to 2 as the Eu coverage increases. With the help of our previous Auger fine-structure analysis of the Pd $M_{4,5}VV$ spectra,[22] we conclude that a mixed Eu-Pd interface has formed as soon as the loss of RHEED patterns is observed. In order to explain the continuous decrease of the Eu mean valence, one has to invoke the formation of more and more divalent Eu sites as the coverage increases (a similar conclusion was given recently by Selås and Raaen[23] from experiments on Eu evaporated on polycrystalline Pd). Thus, the formation of amorphous alloys Eu_xPd_{1-x}, where x is coverage dependent, is strongly suggested. This is supported by the possibility of getting such amorphous alloys over a wide range of concentrations[15] in which a continuous decrease of the Eu mean valence has been observed. In order to verify and emphasize this hypothesis, we now discuss the photoemission results obtained for different Eu coverages: 10, 21, 64, and 122 Å. [Speaking in terms of Θ would be meaningless and thus, we prefer to characterize the Eu coverage by the equivalent Eu thickness (d_{Eu}) as determined by quartz measurements.] These results will be compared to those obtained for the polycrystalline samples $EuPd_y$ ($y=1$, 2, 3, 5). For these thicknesses, Eu is found to be divalent except for the 10-Å deposit for which the Eu mean valence is 2.1.

1. *Valence-band spectra*

The valence-band spectra, for both the different Eu coverages and the polycrystalline compounds, are shown in Fig. 7. For comparison, these spectra have been normalized to the maximum height.

The XPS valence-band spectra of the polycrystalline compounds exhibit a continuous decrease of the bandwidth, associated with a shift toward higher binding energies, as Eu concentration is increased. Such effects have already been observed and described by Fuggle *et al.*[24] for a great variety of Ni and Pd intermetallic compounds and/or alloys. It appears, from such studies, that the interpretation in terms of *d*-band filling is very appropriate. The XPS spectra obtained for the four different Eu coverages behave in the same way, indicating that the 4*d* band of Pd, which is involved in the mixed interface, is filled up as the Eu coverage increases.

A similar behavior is observed on the He I and He II valence-band spectra. Due to the filling of the Pd 4*d* band, the maxima of the density of states (DOS), for the $EuPd_y$ intermetallics, shift to higher binding energies. Here again, the same evolution of the UV spectra is observed in the case of Eu deposition on Pd(111).

These observations complete the previous discussions about both the behavior of the Pd *MVV* Auger spectra and the continuous change of the Eu mean valence as a function of the deposited Eu thickness. It is now tempting to address one of the crucial points of our study, which is to get quantitative information about the concentration of the amorphous Eu_xPd_{1-x} alloys that form at the interface. As discussed below, this can be made by doing simple comparisons between the different valence-band spectra we obtained.

For the 122-Å Eu deposit, it appears that the valence-band spectra compare fairly well with those of the EuPd compound. However, the XPS valence-band spectrum is narrower in the case of the Eu/Pd interface and, as re-

vealed by the He I spectrum, the maximum in the DOS lies at higher binding energy, whereas the Pd 4*d* bandwidth is obviously narrower. Thus, we have to conclude that the amorphous alloy Eu_xPd_{1-x} that forms at the interface has an Eu concentration (x) higher than 0.5. This conclusion assumes that the alloy is homogeneous (i.e., that there is no concentration gradient across the mixed interface). The validity of this assumption will be discussed later in Sec. IV B 3.

For the 64-Å Eu deposit, the XPS and He I spectra can be superimposed on those of the EuPd compound. Then, in that case, the Eu concentration is near 0.5.

For the 21-Å deposit, the situation seems to be more complicated: the XPS bandwidth lies in between that of $EuPd_2$ and $EuPd_3$, but the energy shift compares rather well to the one of $EuPd_3$ or $EuPd_5$. This apparent contradiction is due to a Pd contribution from the substrate

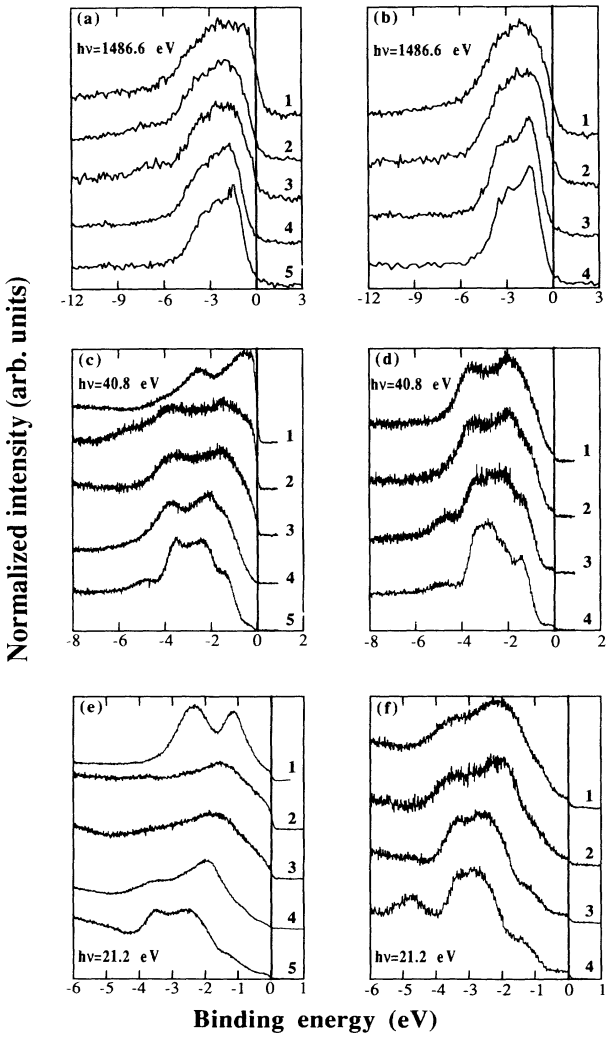

FIG. 7. Valence-band spectra obtained at 1486.6, 40.8, and 21.2 eV. (a), (c), and (e) show spectra for Eu-Pd compounds: (1) Pd(111); (2) $EuPd_5$; (3) $EuPd_3$; (4) $EuPd_2$; (5) EuPd. (b), (d), and (f) show spectra for Eu on Pd(111): (1) 10 Å; (2) 21 Å; (3) 64 Å; (4) 122 Å. The vertical bars indicate the Pd(111) Fermi level.

because the deposited Eu thickness is in the range of the electron mean free path. The further analysis of the Pd 3*d* core-level spectra (see Sec. IV B 2) confirms this assumption. Thus, a better estimation of the alloy concentration may be obtained with the help of the He I spectrum because the electron mean free path is slightly lower than for XPS. In that case, the spectrum is very similar to the one of $EuPd_2$, but with a slightly weaker Pd 4*d* bandwidth and a maximum in the DOS that is at a higher binding energy. Thus, the Eu concentration should be slightly higher than 0.33.

For the 10-Å Eu deposit, the same remarks about the electron mean free path must obviously be taken into account. The only valuable comparison can be made between the He I spectra. The Pd 4*d* bandwidth is a little higher than the one of $EuPd_2$ and thus we may conclude that the alloy concentration should be lower than 0.33 but higher than 0.25 (by reference to the $EuPd_3$ He I spectrum).

Similar comparisons can be made between the He II spectra [Figs. 7(c) and 7(d)], which yield roughly the same conclusions. However, there are differences that may be explained by the fact that with He II radiation we are more sensitive to the surface than with He I or XPS. In particular, the small amount of oxygen contamination, which was always present in the case of the polycrystalline samples, may obscure the conclusions of such comparisons. Nevertheless, the fact that similar conclusions are given by all the three techniques support strongly the formation of homogeneous (in the sense discussed above) Eu_xPd_{1-x} alloys at the interface between Eu and Pd.

2. *Pd 3d XPS core-level spectra*

The Pd 3*d* core-level spectra of the $EuPd_y$ intermetallic compounds [see Fig. 8(b)] again reflect the filling of the Pd 4*d* band: the XPS line becomes more and more symmetrical, whereas it shifts towards the high-binding-energy side with Eu content. The positions of the well-known Pd satellites,[25] relative to the main peak (ΔE_c), are also strongly concentration dependent, as shown in Fig. 8(c) and summarized in Table I. We can see that the parameters of the Pd 3*d* core-level spectra in the case of the Eu/Pd interface behave in the same way for the different Eu deposits, as reported in Fig. 8(a).

In order to get quantitative information, all the $3d_{5/2}$ Pd spectra were fitted using a nonlinear least-square process. A Doniach-Sunjic profile convoluted with an experimental Gaussian resolution (1 eV FWHM) was chosen to represent the theoretical line. No background was subtracted from the experimental data. The natural $3d_{5/2}$ linewidth (γ) was supposed to be the same for all the spectra. With these constraints, the best value for the γ parameter of the Doniach-Sunjic function was found to be 0.24±0.04 eV, in good agreement with earlier published theoretical and experimental data.[26,27]

A good fit of the Pd $3d_{5/2}$ line for the Pd(111) substrate was only achieved by taking into account a second feature, located at 0.40±0.10 eV from the main line on the high-binding-energy side (keeping the linewidth and the asymmetry parameter constant). The relative intensi-

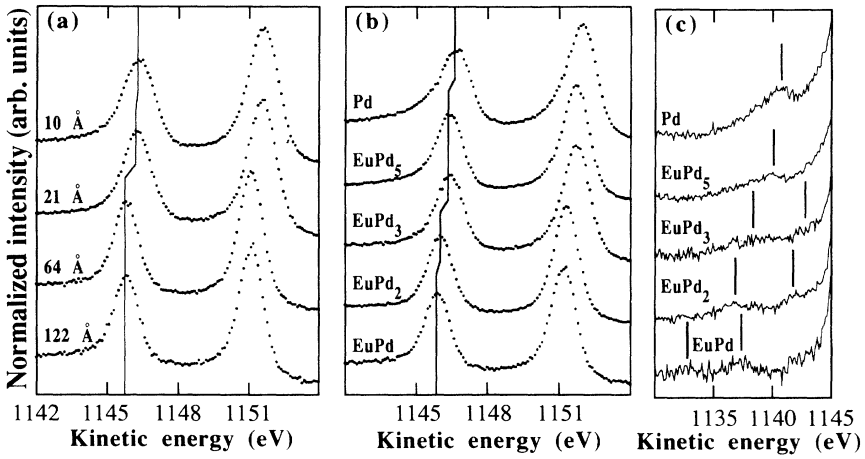

FIG. 8. XPS Pd 3*d* spectra recorded for (a) Eu deposited on Pd(111) at room temperature; (b) Pd(111) and $EuPd_y$ ($y=1, 2, 3, 5$) polycrystalline compounds; (c) Pd 3*d* satellites of the Eu-Pd compounds. The vertical bars indicate the approximative positions of the corresponding $3d_{3/2}$ and $3d_{5/2}$ satellites. For Pd and $EuPd_5$, the $3d_{5/2}$ satellites are obscured by the $3d_{3/2}$ main line.

ty of this second contribution increases significantly when the normal of the sample is tilted by 60° from the direction of the analyzer (i.e., in a more surface-sensitive position), showing that it originates from a surface contribution.[28] This result is in agreement with the work of Erbudak *et al.*[29]

For the 10- and 21-Å Eu deposits, as these thicknesses compare with the Pd 3*d* photoelectron mean free path, it was necessary to superimpose two contributions in the fit: the first one originates from the Pd(111) substrate and the second one from the interface alloy. In those fits, all the parameters concerning the contribution of the Pd substrate were kept constant at their values deduced from the uncovered Pd(111) substrate. For the other cases (64- and 122-Å Eu deposits and polycrystalline compounds), good fits were obtained by taking a single contribution to the XPS Pd $3d_{5/2}$ line. All the results are summarized in Table I.

Direct comparisons between the fit parameters obtained in the case of the intermetallic compounds and those of the Eu/Pd interfaces can be made. As can be seen from Table I, the results are consistent with the con-

TABLE I. Energy and satellites positions of the Pd 3*d* line for the different samples, and electronic parameters deduced from the line fit (see text).

Eu thickness	E_c (eV)[a] Pd $3d_{5/2}$	ΔE_c (eV)[b]	Asymmetry parameter[c]	Intensity ratios[d]
10 Å	1151.6[e]	7.2[e]±0.6	0.15	1.25[f]±0.1
21 Å	1151.55[e]	8.5[e]±0.5	0.14	1.8[f]±0.2
64 Å	1151.2	14.1±0.8	0.13	3.2±0.2
122 Å	1151.1	not measured	0.12	4.3±0.3
Annealing at 820 K	1151.65	9.4±0.6	0.11	1.0±0.2
Compounds				
Pd(111)	1151.9	6.0±0.5	0.20	
$EuPd_5$	1151.7	6.7±0.5	0.16	0.60±0.05
$EuPd_3$	1151.7	7.4±0.9	0.16	0.82±0.05
$EuPd_2$	1151.25	9.3±0.5	0.12	1.29±0.05
EuPd	1151.15	13.1±0.6	0.13	2.92±0.05

[a]Kinetic energy. Uncertainty: ±0.15 eV.
[b]Energy difference between the $3d_{3/2}$ line and the corresponding satellite.
[c]Deduced from the Pd 3*d* line fit. Uncertainty: ±0.01.
[d] 3*d* measured intensity ratios I_{Eu}/I_{Pd} as explained in the text.
[e]Value not corrected for substrate contribution.
[f]Obtained after subtracting the substrate contribution.

clusions obtained from the valence bands, except in the case of the 21-Å Eu deposit where, from the Pd 3*d*, it appears that the Eu concentration should be lower than 0.33.

Concerning the satellite positions relative to the main line (ΔE_c), the agreement is not so good. In fact, such satellites are made of rather different contributions (extrinsic and intrinsic) and extrinsic satellite contributions may be present in the spectra. Indeed, Hillebrecht *et al.*[25] have shown that these extrinsic losses are the predominant part of the satellites in the La-Pd alloys (and more generally in the light rare-earth Pd alloys). These extrinsic losses, like plasmons, at variance with those of intrinsic nature, are not directly associated with the local electronic structure and/or environment. In fact, as it has been discussed at the beginning of Sec. IV B, the continuous valence decrease of Eu led us to suspect that the interface alloys are amorphous. The observation of a diffuse background on the RHEED patterns agrees well with such a hypothesis. It is then tempting to try to correlate the differences observed for the ΔE_c values with the amorphous nature of the alloys that form on the Pd(111) surface. This would imply that amorphous and polycrystalline compounds with the same Eu concentration show different extrinsic losses. Of course, it is somewhat speculative, and deeper studies are needed in order to confirm or disprove this assumption.

3. *Intensity measurements*

A quantitative estimation of the Eu concentration (x) in the mixed interfaces may be given by the measured intensities of the XPS 3*d* core-level spectra. For Pd, the total area (I_{Pd}) of the 3*d* line was measured, including the satellite contributions. For Eu, as the $3d_{3/2}$ line is obscured by the Pd *MVV* Auger lines, the intensity (I_{Eu}) was measured only on the $3d_{5/2}$ spectra. In order to minimize systematic errors due to different sample sizes (especially for the $EuPd_y$ compounds), the intensity ratio I_{Eu}/I_{Pd} was taken as the relevant parameter. In all cases, a Shirley's-type background was subtracted. The results are listed in Table I and plotted in Fig. 9 as a function of Eu thickness.

From these measurements and according to the method described in the Appendix, the Eu concentration was deduced. It is shown in Fig. 10 as a function of the deposited Eu thickness. In all cases, the Eu concentrations we found are in excellent agreement with those expected from the valence-band and Pd 3*d* spectra discussed above. This is an indication that the concentration gradient in these mixed Eu/Pd interfaces is rather small and, as previously observed in RE-TM systems,[30] that an alloy of a given concentration develops at the interface. However, because of the surface sensitivity of the photoemission process, our conclusion about the absence (or the weakness) of a concentration gradient is only relevant for the first ≈ 30 Å beyond the surface sample. Finally, let us mention that, from the results shown in Fig. 10, it is rather difficult to formulate a conclusion about the existence of an upper limit for the Eu concentration at the interface. If it does not exist, this would imply the possibility of finally getting pure europium on the palladium substrate at room temperature.

C. Study of the ordered $EuPd_3$ phase formed at 820 K

As shown by the RHEED and x-ray-diffraction experiments presented in Sec. III, there is a complete reorganization of the Eu/Pd interface when the sample is heated at 820 K after Eu deposition or if the Eu deposition is made directly at high temperature (since the two processes lead to the same results, we shall not distinguish between them in the following). As shown in Fig. 9, the XPS intensities obtained after annealing suggest that the interface properties do not depend anymore on the thickness of the Eu deposit, except perhaps at low coverage (≤ 10 Å). This is fully confirmed by all our photoemission results. For brevity, we shall only present here the results obtained in the case of a 64-Å Eu deposit.

In Fig. 11, the valence-band spectra recorded with Al $K\alpha$, He I, and He II radiations are shown. Now, we must emphasize that direct comparison with the results presented on polycrystalline compounds is no longer possible due to the fact that the interface is ordered. Indeed,

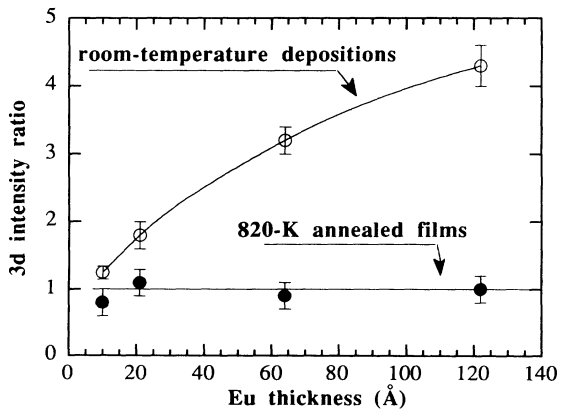

FIG. 9. Measured XPS 3*d* intensity ratios (I_{Eu}/I_{Pd}) (see text). Solid lines are a guide for the eyes.

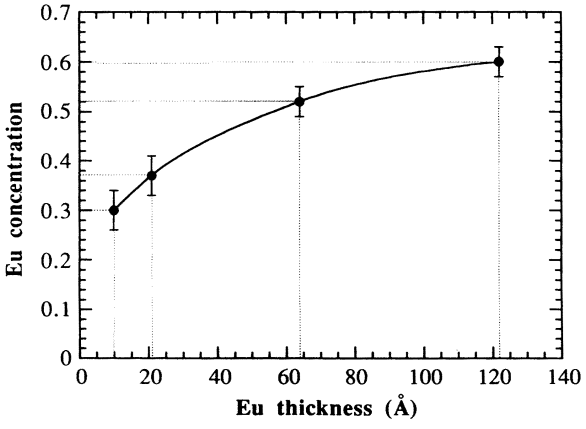

FIG. 10. Eu concentration in the Eu_xPd_{1-x} alloys as a function of the deposited Eu thickness at room temperature (see Appendix). Solid line is a guide for the eyes.

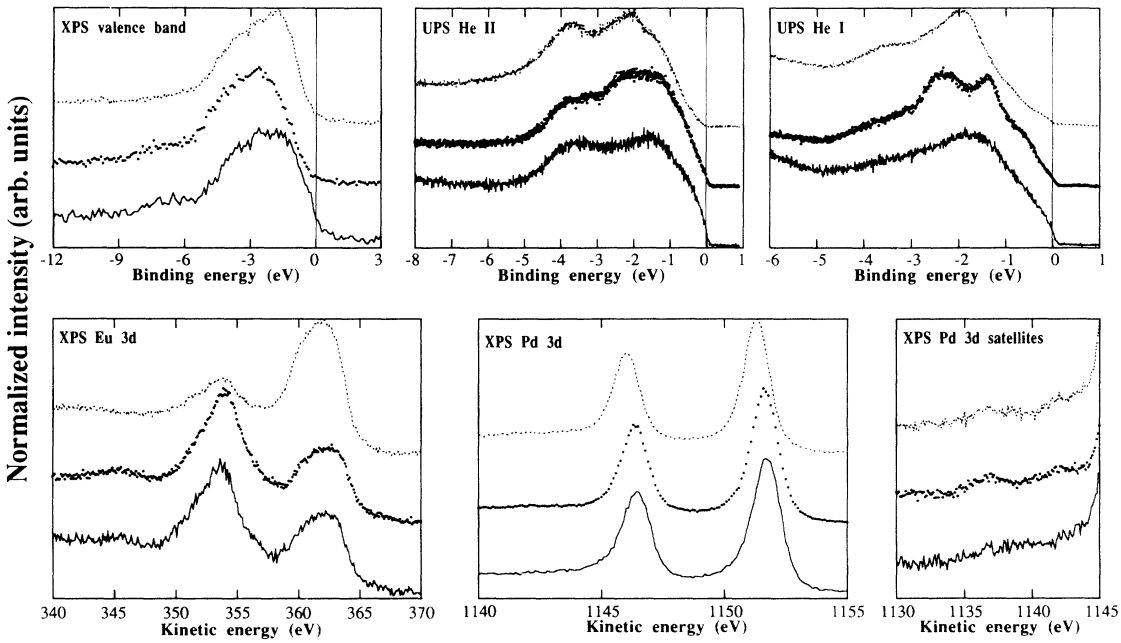

FIG. 11. Photoemission spectra of the annealed interface (64-Å Eu, 820 K, solid points, middle curves) compared with those of the polycrystalline compounds: $EuPd_2$ (dashed lines, upper curves) and $EuPd_3$ (solid lines, lower curves).

despite the large angular acceptance ($\approx 10°$) used in our experiments, angular dispersion is observed[28] when the annealed sample is tilted by 35°. This behavior was not observed for the nonannealed sample and can be related to the observation of two very distinct areas of the Brillouin zone of the ordered compound.

As shown in Fig. 11, the valence-band spectra of the ordered 64-Å Eu interface lie in between $EuPd_2$ and $EuPd_3$. However, the fact that we clearly observed the small bump located at -7-eV binding energy on the XPS spectrum (which was not observed before heating and which is a fingerprint of the trivalent state of Eu) supports the hypothesis of the formation of a trivalent compound. This conclusion is fully confirmed if we compare the Eu $3d_{5/2}$ XPS core-level spectrum of $EuPd_3$ (trivalent compound) to the one of the ordered interface (Fig. 11). A similar conclusion results from the analysis of the Pd $3d$ core-level spectra: the energy position of the XPS line is typical of a trivalent compound.

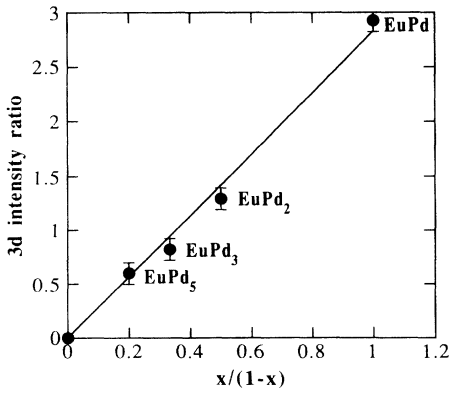

FIG. 12. $3d$ intensity ratios for the Eu-Pd compounds plotted as a function of $x/(1-x)$, where x is the Eu concentration. The solid line is a linear fit which gives the R_0 (2.83) value as discussed in the Appendix.

The intensity ratio deduced from the Eu and Pd $3d$ lines may be affected by photodiffraction effects. Despite this possible phenomenon, the measured values lead to a 26 ± 2 % Eu concentration (i.e., $EuPd_{\approx 2.85}$), which is in excellent agreement with our previous analysis of the x-ray-diffraction data. The fact that the asymmetry factor and the energy position of the satellites are different from those of an $EuPd_3$ polycrystal (Table I) is probably due to the single-crystal state of the sample and also, obviously, to the fact that the interatomic distances in the epitaxial compound are not the same as for the $EuPd_3$ compound as discussed in Sec. III B.

V. CONCLUSION

Numerous experimental techniques have been used in order to determine both the electronic and the crystallographic properties of Eu/Pd interfaces. All our results agree well with the conclusion that interdiffusion between europium and palladium plays the essential role in the properties of these Eu/Pd interfaces. The main conclusion of our study is obviously that a well-defined intermetallic compound can be stabilized epitaxially at the interface on a large scale.

Usually, epitaxy was searched in systems where the diffusion between the two elements was as small as possible in order to avoid disorder. Here, on the contrary, we take benefit of the diffusion between europium and palla-

dium in order to induce some kind of solid-phase epitaxy. This process is already used in the realization of semiconductor superlattices but, to our knowledge, it is the first time that such a process has been obtained for metallic systems. We believe that our study opens the possibility of realizing some additional kind of metallic superlattices. Experiments on RE-Fe systems, which are very interesting for their magnetic properties, are now in progress.

ACKNOWLEDGMENTS

It is a pleasure to acknowledge Dr. J. P. Kappler and G. Schmerber for providing us with the $EuPd_y$ polycrystalline compounds. We are indebted to Professor M. Piecuch and Professor J. Protas and Dr. E. Beaurepaire, Dr. B. Carrière, and Dr. S. Andrieu for numerous discussions concerning this work. The Laboratoire de Physique des Solides is "Unité Associée du Centre National de la Recherche Scientifique No. 155." The Laboratoire mixte CNRS Saint Gobain is "Unité Mixte du Centre National de la Recherche Scientifique No. 37." The Laboratoire de Microstructures et de Microélectronique is "Unité Propre du Centre National de la Recherche Scientifique No. 20." The Laboratoire Maurice Letort is "Unité Propre du Centre National de la Recherche Scientifique No. 6851."

APPENDIX: DERIVATION OF THE ALLOY CONCENTRATION FROM THE XPS MEASUREMENTS

We start from a homogeneous alloy Eu_xPd_{1-x} of thickness d, lying on the Pd(111) surface. In that simple case the ($3d$) XPS intensities of Pd and Eu are given by

$$I_{Pd}=(1-x)I^0_{Pd}\left[1-e^{-\frac{d}{\lambda_{Pd}}}\right]+I^0_{Pd}e^{-\frac{d}{\lambda_{Pd}}}$$

and

$$I_{Eu}=xI^0_{Eu}\left[1-e^{-\frac{d}{\lambda_{Eu}}}\right],$$

where λ_{Pd} and λ_{Eu} are the electron mean free paths (EMFP) related to the $3d$ lines of Pd and Eu, respectively. For simplicity, we suppose that the EMFP depends only on the kinetic energy of the emitted electrons (Pd $\approx$1150 eV, Eu $\approx$360 eV). We assume that λ_{Pd} is two or three times more important than λ_{Eu}, and λ_{Eu} lies between 4 and 10 Å.[31] This range of EMFP is large enough to ensure a good estimation of the error about the wanted x concentration.

I^0_{Eu} and I^0_{Pd} are the $3d$ intensities of the pure elements. The ratio of these two quantities is found with the help of the reference compounds as indicated below. The two preceeding relations lead to the formula

$$R=\frac{I_{Eu}}{I_{Pd}-I^0_{Pd}e^{-(d/\lambda_{Pd})}}=\frac{I^0_{Eu}}{I^0_{Pd}}\frac{x}{1-x}\frac{1-e^{-(d/\lambda_{Eu})}}{1-e^{-(d/\lambda_{Pd})}}.$$

1. Case of a thick Eu_xPd_{1-x} alloy (64- and 122-Å Eu deposits). In this case, the exponential terms are neglected, and we get

$$R=\frac{I_{Eu}}{I_{Pd}}=R_0\frac{x}{1-x},$$

where R_0 may be directly obtained from the measured intensities of the polycrystalline $EuPd_y$ compounds. The quasilinear variation of R as a function of $x/(1-x)$ plotted in Fig. 12 shows that the measured intensity ratios are not greatly affected by the drastic changes observed in the $3d$ line shapes for both europium and palladium.

Since we know R_0, we then can find the x value for each Eu deposit by measuring the experimental R quantity.

2. Case of a thin Eu_xPd_{1-x} alloy (10- and 21-Å Eu deposits). Here, the situation is more complicated because the experimentally unknown d value compares with the EMFP, and we cannot neglect the exponential terms. In order to determine the concentration x, we proceed in two steps. In a first step, we remove the Pd(111) contribution from the total Pd intensity by fitting the Pd $3d$ line as indicated in Sec. IV B 3 and we get the experimental R ratio. In a second step, we express the thickness d as a function of x and all the known parameters; a simple calculation yields

$$d=\frac{d_0}{x}\frac{D_{Eu}}{M_{Eu}}\frac{xM_{Eu}+(1-x)M_{Pd}}{xD_{Eu}+(1-x)D_{Pd}},$$

where d_0 is the thickness of the Eu deposit, M_{Eu}, M_{Pd} and D_{Eu}, D_{Pd} are the atomic weight and the density of europium and palladium, respectively. A Vegard law is supposed to be valid to approximate the unknown alloy density. By varying the EMFP in the previously defined ranges, one can now calculate the theoretical expression of R as a function of x. The comparison with the experimental R value gives us the desired concentration.

[1] I. Chorkendorff, J. Kofoed, and J. Onsgaard, Surf. Sci. **152/153**, 749 (1985).
[2] I. Chorkendorff, J. Onsgaard, J. Schmidt-May, and R. Nylhom, Surf. Sci. **160**, 587 (1985).
[3] J. N. Andersen, J. Onsgaard, A. Nilsson, B. Eriksson, E. Zdansky, and N. Mårtensson, Surf. Sci. **189/190**, 399 (1987).
[4] A. Nilsson, B. Eriksson, N. Mårtensson, J. N. Andersen, and J. Onsgaard, Phys. Rev. B **38**, 10 357 (1988).
[5] J. N. Andersen, O. Björneholm, M. Christiansen, A. Nilsson, C. Wigren, J. Onsgaard, A. Stenborg, and N. Mårtensson, Surf. Sci. **232**, 63 (1990).
[6] Å. Fäldt and H. P. Myers, J. Magn. Magn. Mater. **47** and **48**, 225 (1985).
[7] A. Stenborg and E. Bauer, Surf. Sci. **185**, 394 (1987).

[8]A. Ciszewski and A. J. Melmed, J. Phys. (Paris) Colloq. **45**, C9-39 (1984).
[9]Å, Fäldt, D. K. Kristensson and H. P. Myers, Phys. Rev. B **37**, 2682 (1988).
[10]H. Homma, K. Y. Yang, and I. K. Schuller, Phys. Rev. B **36**, 9435 (1987).
[11]C. Gu, X. Wu, C. G. Olson, and D. W. Lynch, Phys. Rev. Lett. **67**, 1622 (1991).
[12]E. Beaurepaire, B. Carrière, P. Légaré, G. Krill, C. Brouder, D. Chandesris, and J. Lecante, Surf. Sci. **211/212**, 448 (1989).
[13]R. M. Nix, R. W. Judd, and R. M. Lambert, Surf. Sci. **215**, L316 (1989).
[14]C. Rau, C. Jin, and M. Robert, Phys. Lett. A **138**, 334 (1989).
[15]D. Malterre, A. Siari, P. Delcroix, J. Durand, G. Krill, and G. Marchal, J. Magn. Magn. Mater. **63/64**, 521 (1987).
[16]T. Gourieux, Thèse de l'Université Nancy I en Science des Matériaux (1990).
[17]M. C. Joncour, Spectra 2000 **143**, 63 (1989).
[18]W. J. Bartels, J. Vac. Sci. Technol. B **1**, 338 (1983).
[19]C. P. Flynn, Mater. Res. Bull. June 1991, 30.
[20]I. R. Harris and G. Longworth, J. Less-Common Met. **23**, 281 (1971).
[21]Steven G. Louie, Phys. Rev. Lett. **42**, 476 (1979).
[22]F. Bertran, T. Gourieux, G. Krill, M. Alnot, J. J. Ehrhardt, and W. Felsch, Surf. Sci. **245**, L163 (1991).
[23]T. Ø. Selås and S. Raaen, J. Phys. Condens. Matter **2**, 7679 (1990).
[24]J. C. Fuggle, F. U. Hillebrecht, R. Zeller, Z. Zolnierek, P. A. Bennet, and Ch. Freiburg, Phys. Rev. B **27**, 2145 (1982).
[25]F. U. Hillebrecht, J. C. Fuggle, P. A. Bennett, Z. Zolnierek, and Ch. Freiburg, Phys. Rev. B **27**, 2179 (1982).
[26]O. Keski-Rahkonen and M. O. Krause, At. Data. Nucl. Data Tables **14**, 139 (1974).
[27]F. Antonangeli, A. Balzarotti, A. Bianconi, P. Perfetti, P. Ascarelli, and N. Nitisco, Solid State Commun. **21**, 201 (1977).
[28]F. Bertran, Thèse de l'Université de Nancy I en Science des Matériaux (1992).
[29]M. Erbudak, P. Kalt, L. Schlapbach, and K. Bennemann, Surf. Sci. **126**, 101 (1983).
[30]C. Brouder, G. Krill, P. Guilmin, G. Marchal, E. Dartyge, A. Fontaine, and G. Tourillon, Phys. Rev. B **37**, 2433 (1988).
[31]M. P. Seah and W. A. Dench, Surf. Interf. Anal. **1**, 2 (1979).
[32]The method employed to derive the Eu mean valence was the same for 3*d* and 4*d* photoemission: by using a least-square fit, each spectrum was decomposed into a linear combination of trivalent and divalent components. The pure divalent (trivalent) reference component was the spectrum of EuPd (oxydized $EuPd_5$ in order to cancel the divalent surface contribution). Slight variations in the energy scale of reference spectra were included in the fits in order to simulate the chemical-shift effect. Such a procedure allows the determination of the mean valence: $v=2+I(3^+)/[I(2^+)+I(3^+)]$ with an accuracy of 3%.

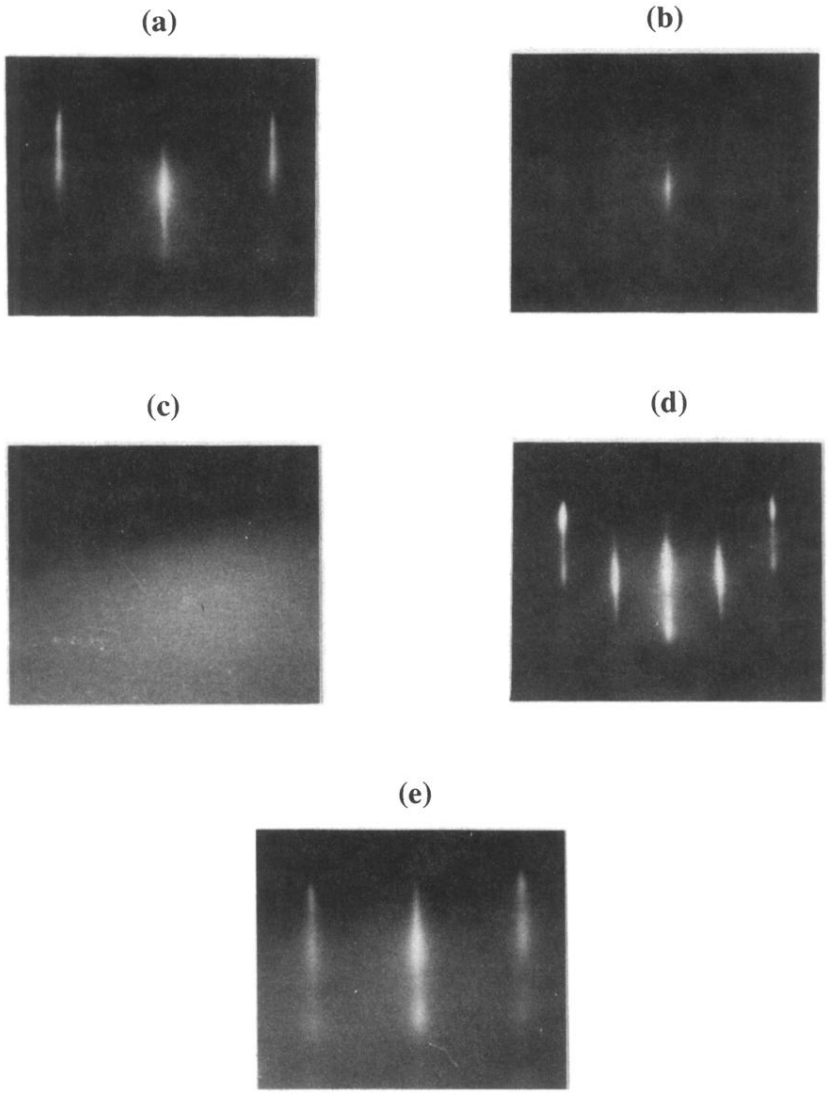

FIG. 1. RHEED patterns in the [01$\bar{1}$] real-space direction. (a) pure Pd(111). (b) 3-Å Eu deposited at RT. (c) Disappearance of RHEED patterns when the Eu deposit at RT is higher than 5 Å. (d) 190-Å Eu deposited at RT and annealed for 2 min at 1000 K. (e) 40-Å Pd deposited on the 190-Å reconstructed interface and annealed for 2 min at 700 K.